The effects of planetary obliquity on the Hadley cell

Alexander Paterson*

University of Exeter, Exeter, UK

Geoffrey Vallis

University of Exeter, Exeter, UK

Corresponding author address: CGAFD, University of Exeter, Exeter, United Kingdom

E-mail: ap587@exeter.ac.uk

ABSTRACT

Placeholder abstract text.

1. Introduction

Note to assessors: This is an incomplete draft of a paper that I am actively working on. Before you read through (if it's a while since the upload) I may have a more up-to-date copy avaliable if you email me! I am currently working on wrangling the data into a conclusion, with some more heavy duty analysis and engagement with some theory. Thank you! - Alex

2. Model

We aim to use a simple, flexible GCM to simulate variations in planetary and atmospheric parameters, with emphasis on obliquity. We then wish to use this model to study how the Hadley cell responds to these conditions, which could plausibly be found on an exoplanet in the coming years. To this end we use Isca, a derivative of GFDL's FMS idealized aquaplanet model (cite model paper). Within this framework, we use a dry atmosphere forced by Newtonian relaxation to a prescribed equilibrium temperature field. The forcing we use is a new method following a more physically motivated path than is typically used [cite].

This method involves 5 main steps:

1. Calculation of the incoming solar radiation at each latitude. We use a diurnally averaged solar flux, S, following the method of **?**:

$$S(\phi) = \frac{q_0}{\pi}(H \sin\phi \sin\delta + \cos\phi \cos\delta \sin H), \tag{1}$$

where q_0 is the bolometric solar flux. H is the radian half-day length which is 0 for perpetual night and π for perpetual day. ϕ is the latitude and δ is solar declination, in the range $-\delta_0 < \delta < \delta_0$ where δ_0 is the planet's obliquity.

2. Use the insolation at each latitude to calculate a top-of-atmosphere temperature. This uses a simple radiative equilibrium model for the vertical temperature structure. The balance of

albedo adjusted incoming shortwave with outgoing longwave results in a top-of-atmosphere temperature of:

$$T_t(\phi) = \left(\frac{S(\phi)(1-A)}{2\sigma}\right)^{\frac{1}{4}}, \tag{2}$$

where σ is the Stephan-Boltzmann constant and the factor of 2 on the denominator is the difference between emitting and top-of-atmosphere temperature.

3. The vertical structure is simplified into two layers: a troposphere with a uniform lapse rate, and a stratosphere with no change in temperature. The height of the boundary between these layers is determined by performing a convective adjustment to the radiative equilibrium profile, see **?**.

——— More detail about this derivation ———

We assume that convection is efficient such that it establishes a convectively neutral lapse rate, Δ, and that it equalizes the ground and surface layer temperatures. We can then solve numerically for the tropopause height, or use the following approximate analytic solution:

$$H_T(\phi) = \frac{1}{16\Gamma}\left(CT_T(\phi) + \sqrt{C^2T_T(\phi)^2 + 32\Gamma\tau_s H_a T_T(\phi)}\right) \tag{3}$$

where T_T is the tropopause/top of atmosphere temperature, C = log4, Γ is the lapse rate, τ_s is the optical depth at the surface, and H_a is the scale height of the absorber in the atmosphere (water vapour on Earth). Typical Earth values of these parameters are: $\Gamma = 6.5Kkm^{-1}$, $\tau_s = 5$, and $H_a = 2km$. The full derivation of this equation is available in **?** [GV2017].

4. A constant lapse rate is used to calculate troposphere temperatures down to the surface, with a stratosphere of constant temperature at each latitude.

5. The effects of surface heat capacity are modelled by using the flux from the insolation direct temperature, T_{insol}, to force the equilibrium temperature, T_{eq}. The heat capacity, c, is defined

by a certain depth of a global mixed layer ocean.

$$c\frac{\partial T_{eq}(\phi)}{\partial t} = \sigma\left(T_{insol}(\phi)^4 - T_{eq}(\phi)^4\right). \tag{4}$$

The entire atmospheric column temperature is therefore shifted to simulate the moderating effect of a heat absorbing surface layer. The entire column is shifted for simplicity, with the assumption that convection quickly brings the temperature profile in the troposphere back to the specified lapse rate.

The stratosphere is left at a constant temperature as to not make assumptions about its structure, while keeping some delineation at the tropopause. The constant temperature approximates the vertical structure in the upper atmosphere from a grey radiative balance model.

a. Experimental setup

Details about my particular experiments aka how i got the results below.

3. Results

Obliquity only effects the seasonal distribution of incoming solar radiation. The total energy received by the planet remains constant throughout these experiments. As obliquity is increased, the planet experiences stronger seasons, until at 90 degrees obliquity where each hemisphere sees a 'polar winter' where the sun never rises for many days. Figure c shows the annual mean and seasonally averaged incoming solar radiation. Of note is the change from the location of peak insolation being at the equator to the poles at 54 degrees obliquity. Due to the strong seasonal effects on planets with high obliquities it is necessary to look at the seasonal rather than annual mean to avoid washing out the true behaviour. Figure cb) shows the mean insolation over the solstice period, defined as one month either side of the solstice. This strong effect of the polar day

is clearly seen. At an obliquity of 75 degrees the insolation peaks at xxW/M^2 at the pole rather than xxW/m^2 at the equator for an Earth-like obliquity.

a. Obliquity climatology

Now we will examine the effects of this on the basic climatology of the planet. First looking at the annual mean followed by the solstice mean for full eddy-permitting and axisymmetric models.

At an obliquity of 30 degrees we observe a regime similar to that of the Earth (Fig: c). There is a wide equatorial region of relatively constant temperature, before dropping 20K to the poles. This temperature gradient is part of the the observed circulation structure. There are Hadley cells reach to around 30 degrees of latitude off the equator and weaker eddy-driven Ferrel cells extending from there to around 70 degrees. We also observe a small, weak polar cell in the lower atmosphere. In the zonal wind field we see a westerly jet in each hemisphere with two peaks. The first, a thermally driven jet, located higher in the troposphere and centered at the edge of the Hadley cell. The second, an eddy driven jet, in the middle of the Ferrel cell which reaches down towards the surface at approximately 60 degrees latitude. The jets are not vertically bounded as this model does not include a temperature gradient reversal in the stratosphere.

If we increase the obliquity to 60 degrees we see a very different temperature structure. The annual mean equator-to-pole temperature gradient is reversed, and much lower as the poles are now the warmest latitudes. The lower branch of the Hadley cell has weakened compared with the lower obliquity case. The Ferrel cells have narrowed, now ending at approximately 50 degrees latitude. Overall the circulation in the annual mean is significantly weaker, the meridional mean mass overturning streamfunction is half as intense across the atmosphere. There are no westerly jets present as the strong seasonal effects are masking the jets when the annual mean is taken.

We have also run the same planet under axisymmetric conditions. Here we only allow wave number zero in the spectral model, so no eddies are permitted. In this model the climate differs in a few key ways. [][][]

b. Seasonal effects

To actually understand how the changing obliquity is affecting the climate, we need to examine the seasonal effects in more detail. Figure c shows the solstice mean for the experiments detailed in Figure c. The solstice period here is defined as the time period one month either side of the solstice. In our 30 degree obliquity experiment the offset heating results in a temperature field maxima offset from the equator by approximately 25 degrees. This is caused by the heat capacity of the model moderating the seasonal shift. The mass streamfunction shows a cross-equatorial winter Hadley cell paired with a very weak summer cell. The latitude of the ascending branch of the winter Hadley cell does not align with the latitude of maximum temperature; we explore the reasons behind this in section xx. The westerly jet latitudes are fairly unchanged from the annual mean case, the main difference between them being their relative strengths. The winter hemisphere jet is much stronger, associated with the strong Hadley and Ferrel cells. The 30 degree obliquity experiment produces a seasonal climate similar to that of other idealised models of Earth xx. At 60 degrees obliquity, Figure cb), the temperature maxima is now located at the pole. This is consistent with predictions from the insolation equation. Past 21 degrees obliquity the insolation maxima for the season is at the pole. There is now one global circulation cell, the winter cross-equatorial Hadley cell. Interestingly it is of similar size and intensity as the Hadley cell at 30 degrees obliquity, while the temperature structure has changed significantly. We look in detail at the reasons for this in section xx. An eddy driven westerly jet is not present at higher obliquities. Instead we only see the thermally driven upper jet centered at the edge of the Hadley cell. In the

summer hemisphere we see an easterly jet with a maxima on the up-welling branch of the Hadley cell. This is a thermal jet caused by the reversed, now pole-equator, temperature gradient.

Axisymmetric solstice description

c. Surface temperature effects

Figure c shows the annual mean equator-to-pole temperature difference for eddy permitting and antisymmetric models. Both cases feature a clear negative relationship between these values. At smaller obliquities the axisymmetric runs have a much larger equator-to-pole difference as there are no eddies providing poleward heat transport. Past 54 degrees in the 3D case, we see a negative temperature gradient. Here the poles are warmer than the equator, as we saw in the field slices (Fig c). At very hight obliquities, greater than 60 degrees, we see the axisymmetric model and 3D have essentially the same values. This is further evidence to the reduced role of eddies at high obliquities - with the climate dominated by a single thermally direct overturning Hadley cell.

The strength of the solstice Hadley cell is observed to increase consistently from 0 to 90 degrees obliquity. This is in contrast with the annual mean cell which decreases in strength, with an exception at 30 degrees. At 30 degrees there is a strong winter cell which is still largely concentrated in the winter hemisphere. At high obliquities, this winter cell is centered over the equator, and so in the annual mean is largely cancelled out.

Acknowledgments. Start acknowledgments here.

References

LIST OF FIGURES

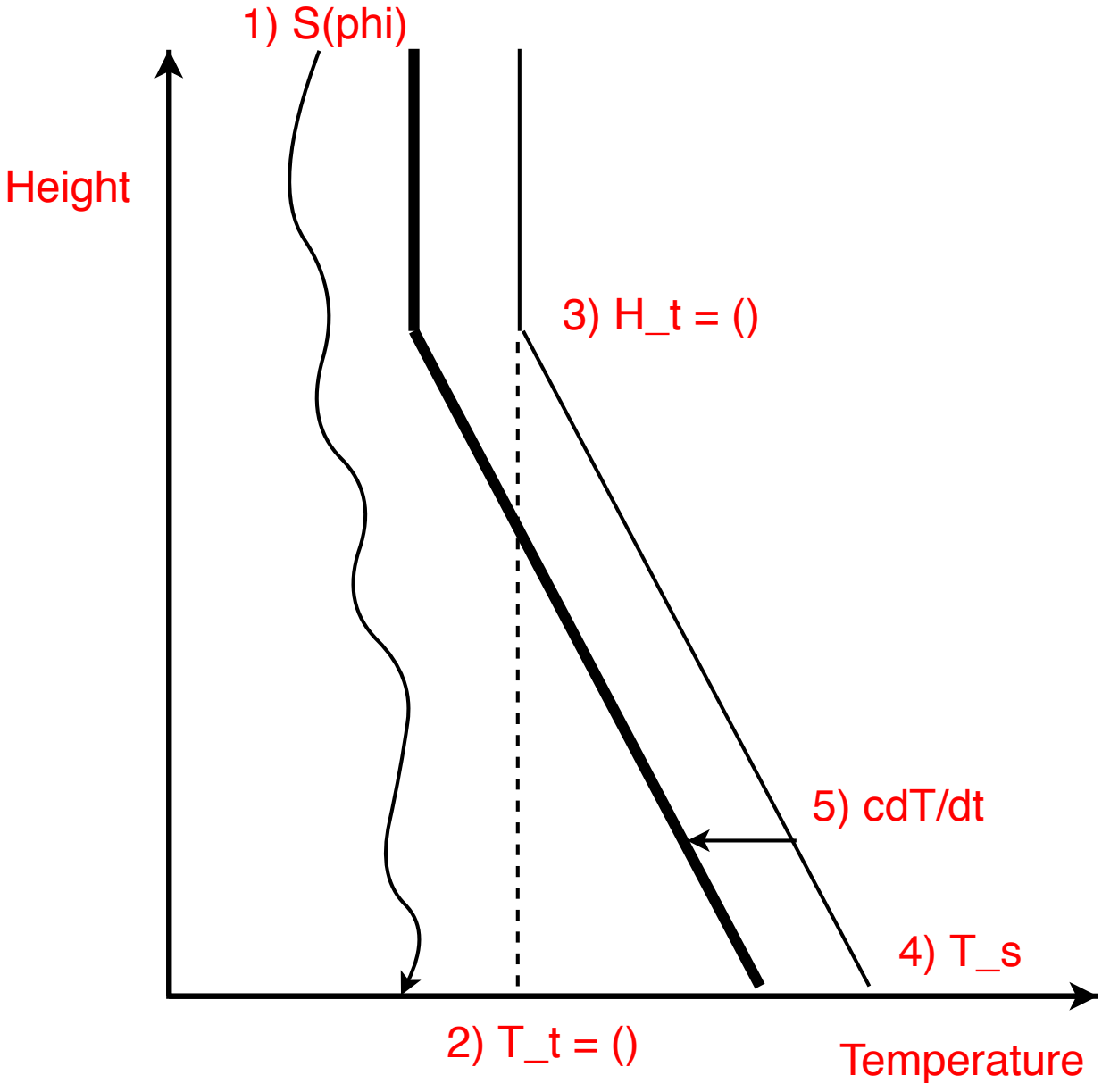

FIG. 1. Diagram of model method

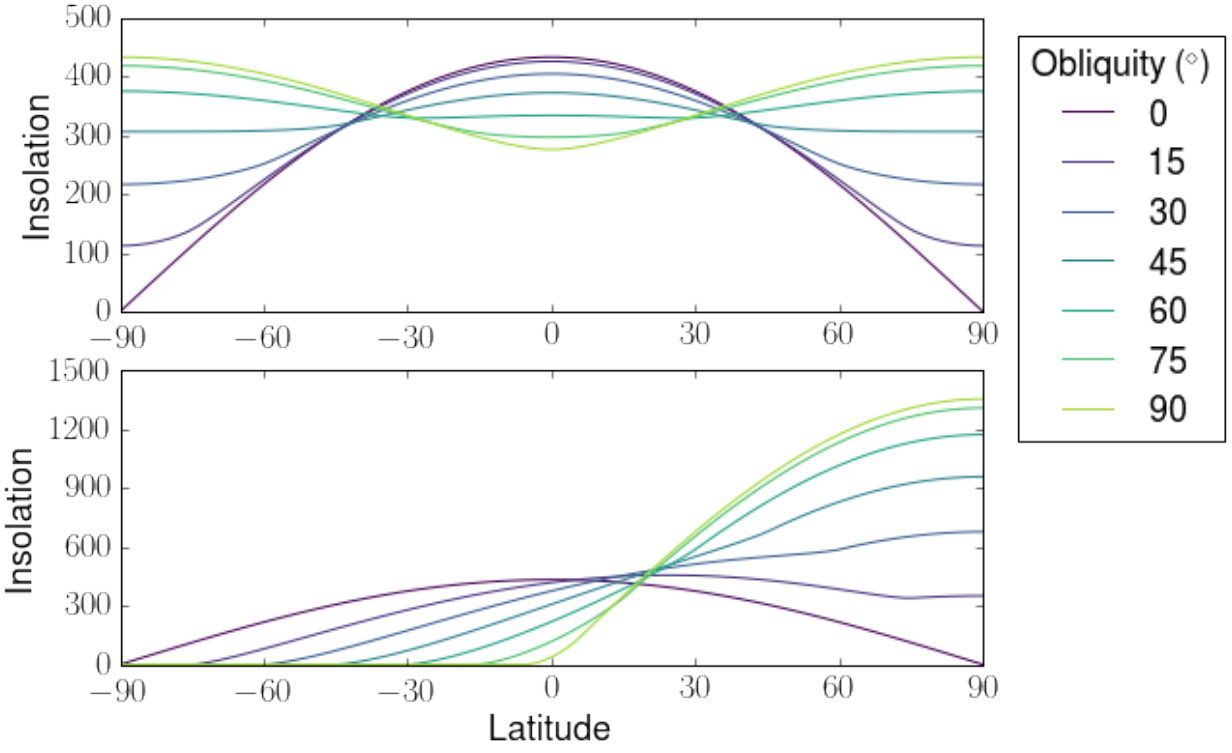

FIG. 2. Top: Annual mean top of atmosphere insolation for obliquities from 15 degrees to 90 degrees. Bottom: Top of atmosphere insolation on the solstice for the same planetary obliquities.

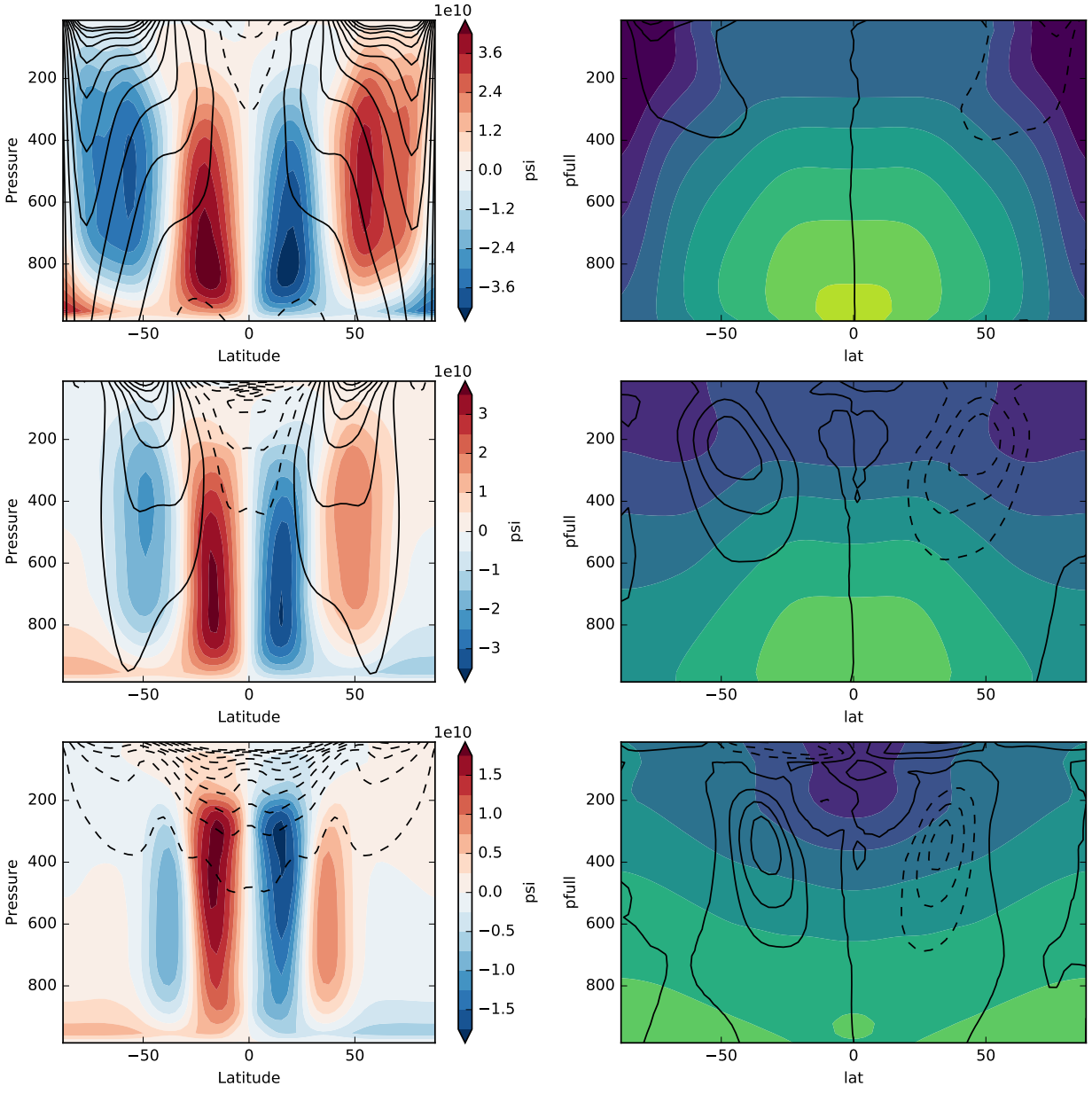

172 FIG. 3. Zonal, annual mean circulation for a series of model runs with obliquity 0° (top), 30° (middle) and
173 60° (bottom). Left: Mass streamfunction (colours) and zonal wind (contours). Right: Temperature (colours) and
174 meridional eddy-momentum flux, $\bar{u'v'}$ (contours).

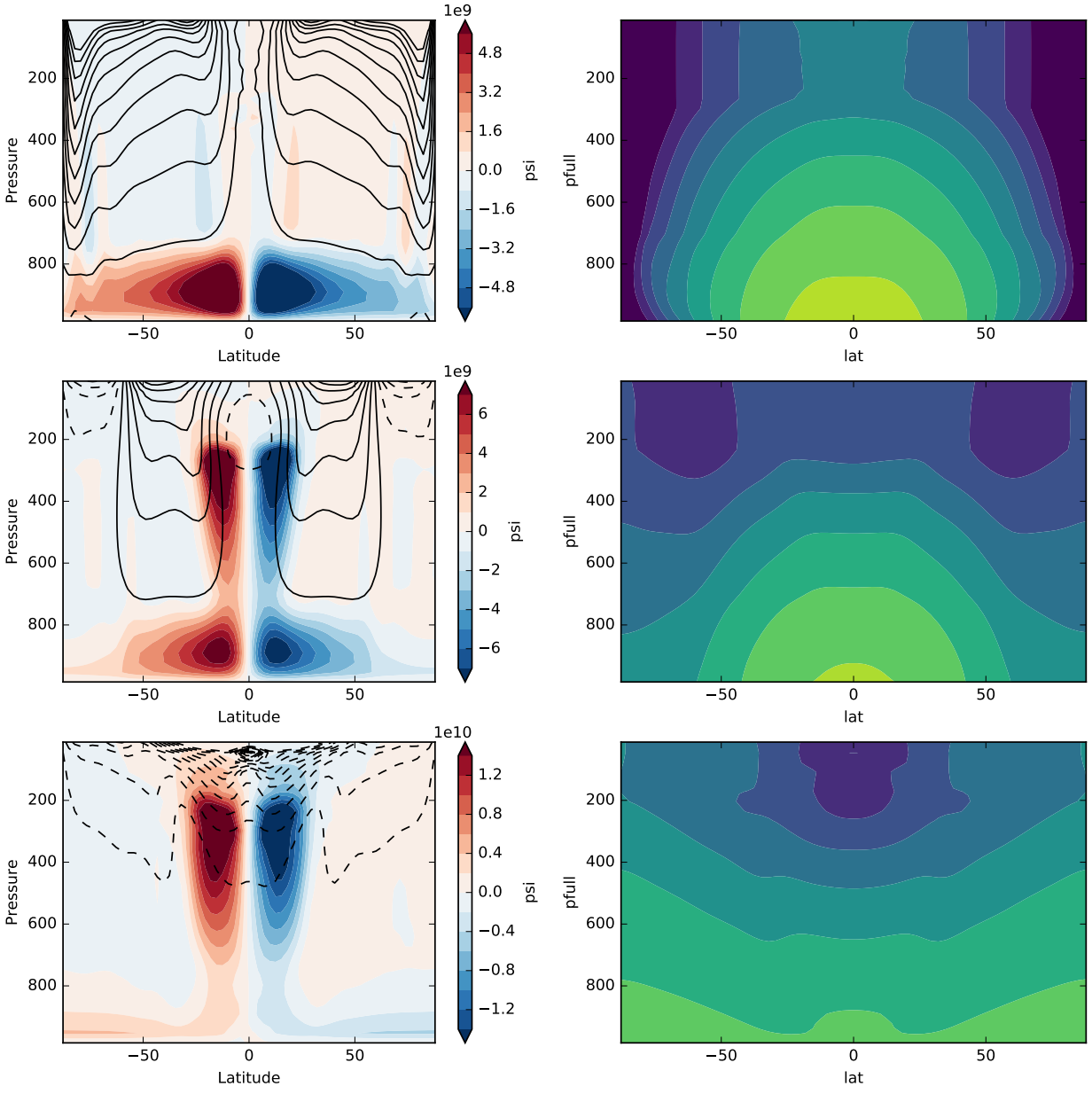

175 FIG. 4. Zonal, annual mean circulation for a series of axisymmetric model runs with obliquity 0° (top), 30°
176 (middle) and 60° (bottom). Left: Mass streamfunction (colours) and zonal wind (contours). Right: Temperature
177 (colours) and meridional eddy-momentum flux, $\bar{u'v'}$ (contours).

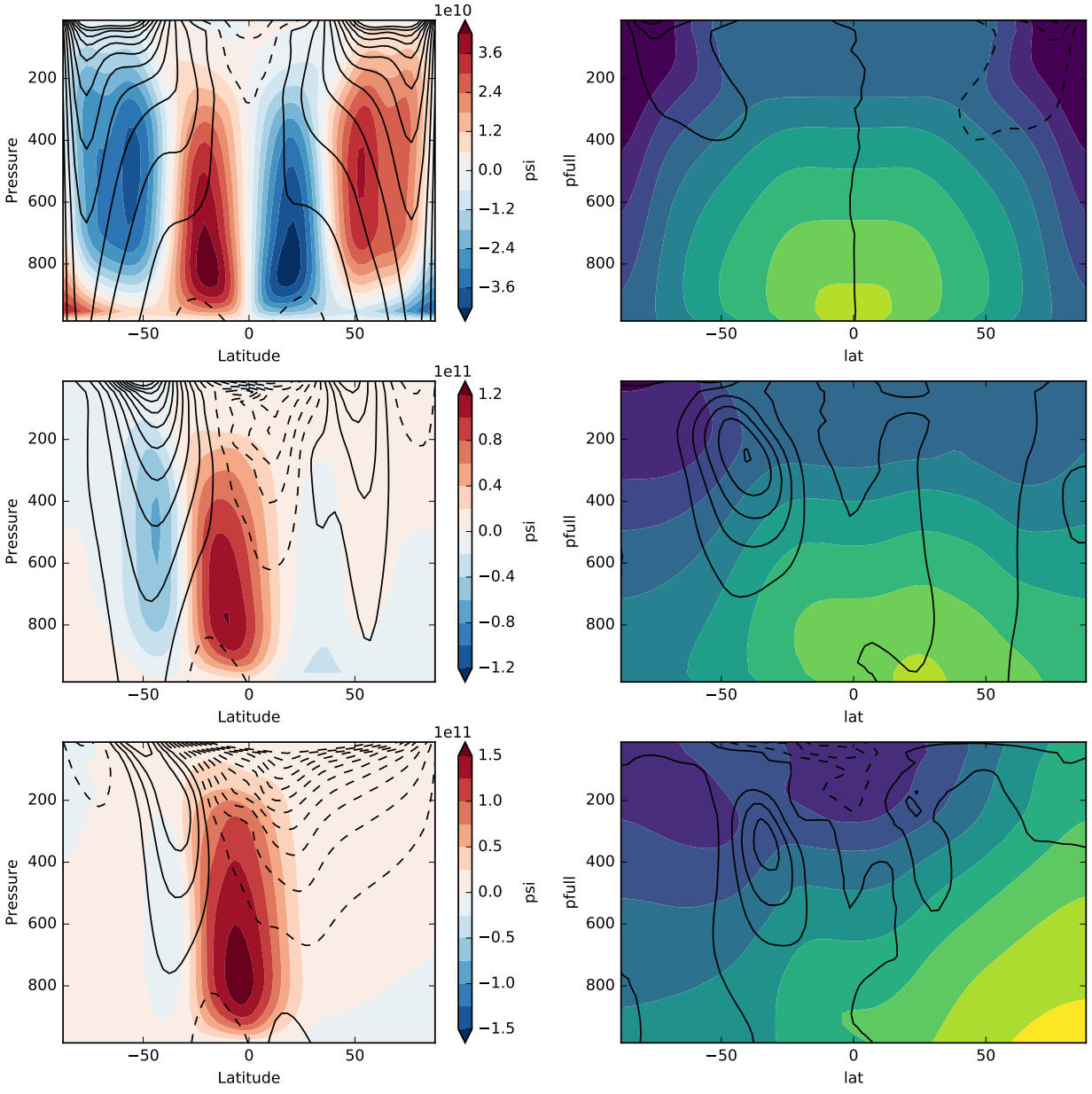

FIG. 5. Zonal, solstice mean circulation for a series of model runs with obliquity 0° (top), 30° (middle) and 60° (bottom). Left: Mass streamfunction (colours) and zonal wind (contours). Right: Temperature (colours) and meridional eddy-momentum flux, $\bar{u'v'}$ (contours).

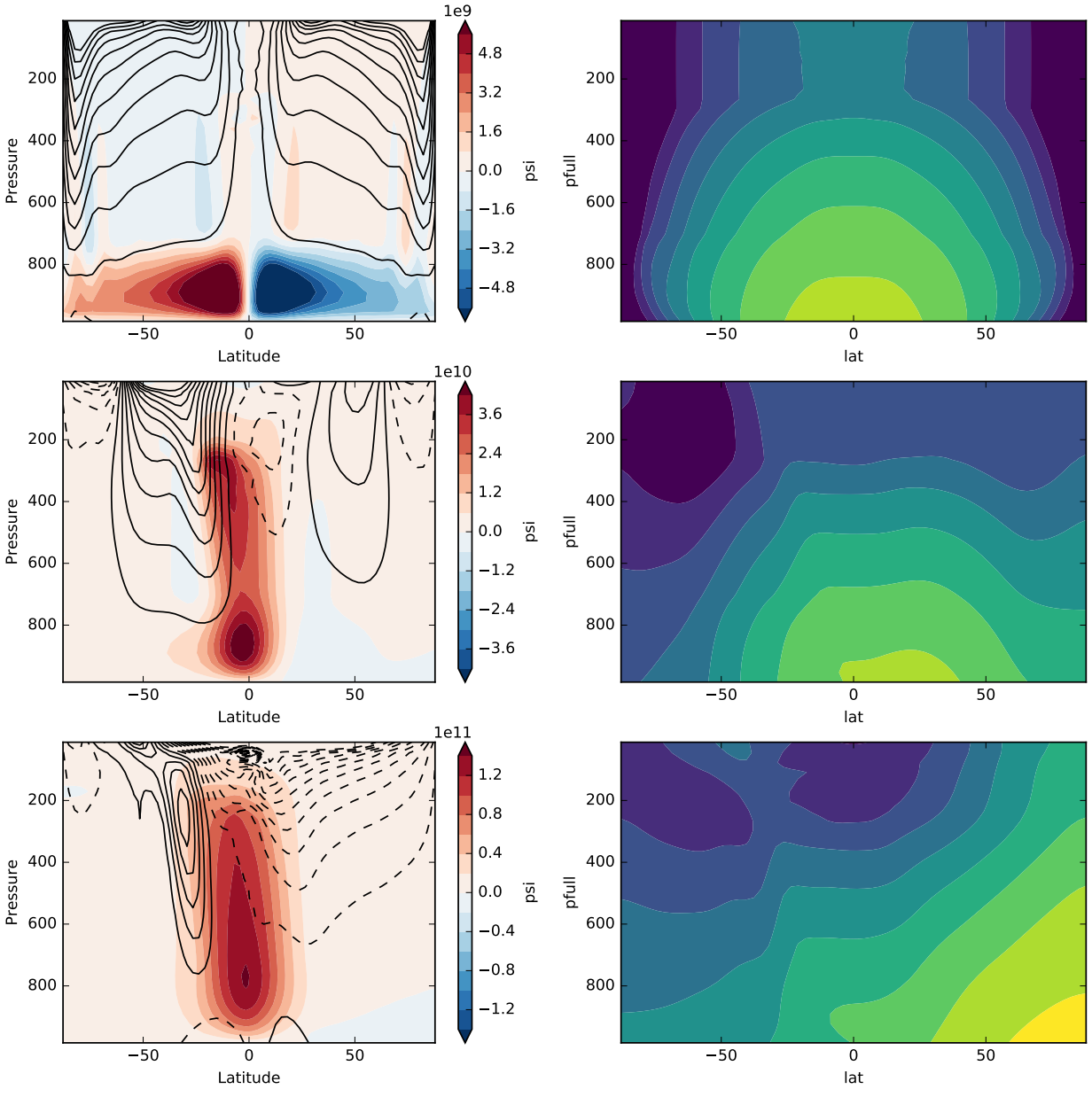

181 FIG. 6. Zonal, solstice mean circulation for a series of axisymmetric model runs with obliquity 0° (top), 30°

182 (middle) and 60° (bottom). Left: Mass streamfunction (colours) and zonal wind (contours). Right: Temperature

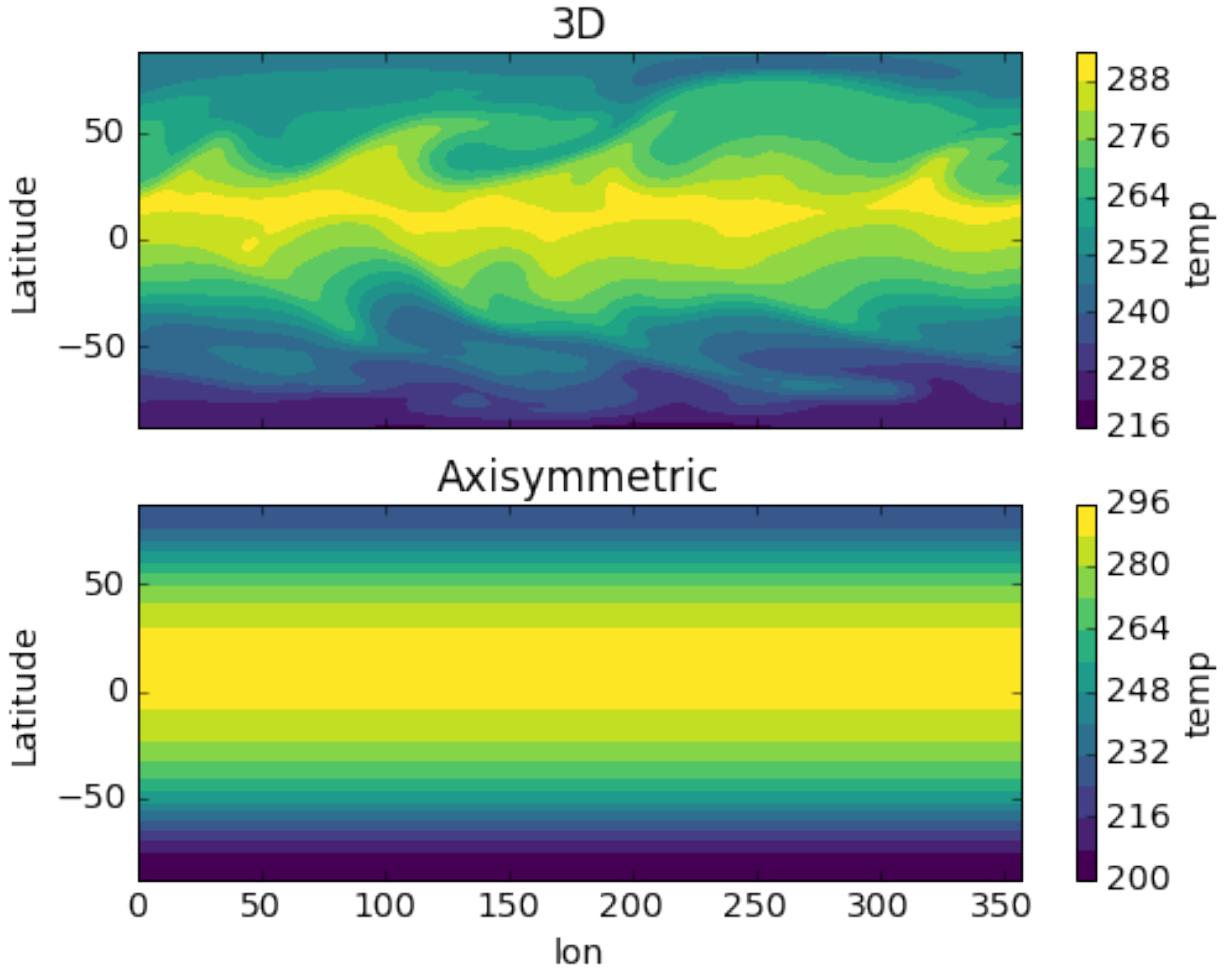

FIG. 7. Surface temperatures at the solstice for 3D and axisymmetric model runs at 15° obliquity.

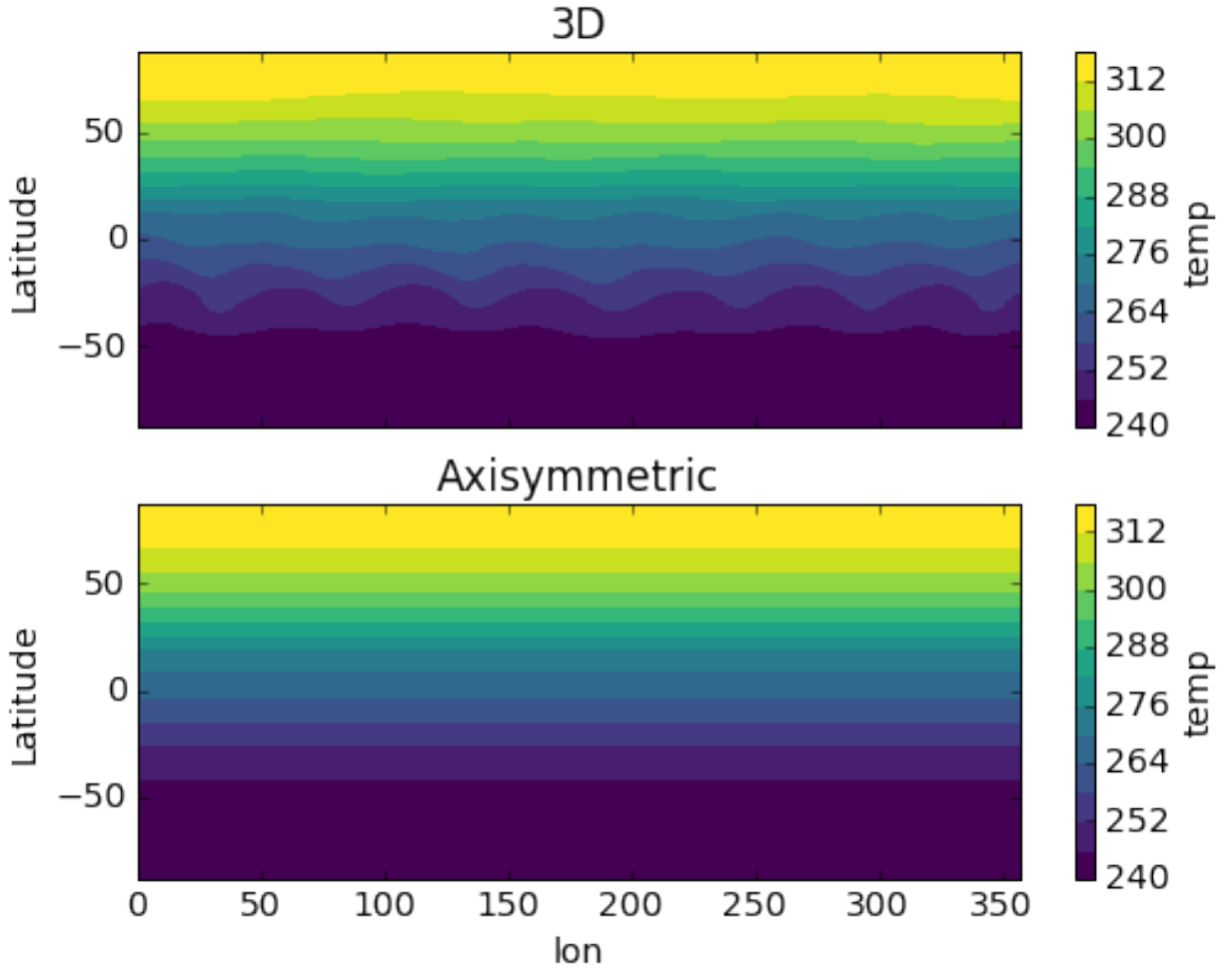

FIG. 8. Surface temperatures at the solstice for 3D and axisymmetric model runs at 60° obliquity.

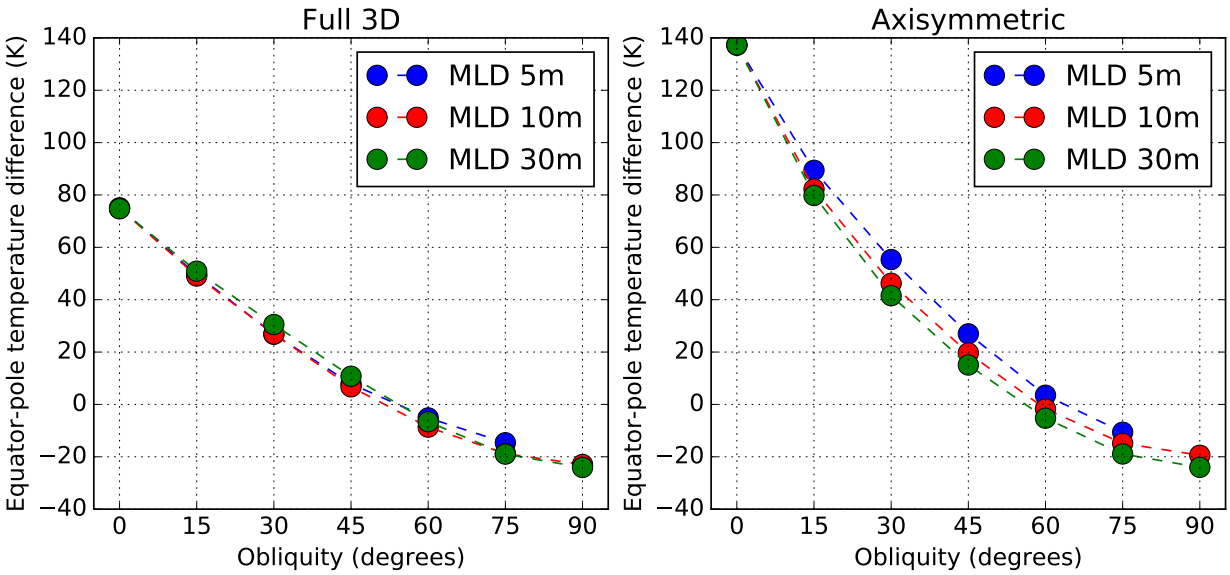

FIG. 9. Annual mean equator-to-pole temperature difference for full 3D eddy permitting, and axisymmetric obliquity variations. Note that the temperature difference is negative for obliquities greater than around 50 degrees. Past this point the poles are warmer than the equator due to the intense polar summer.

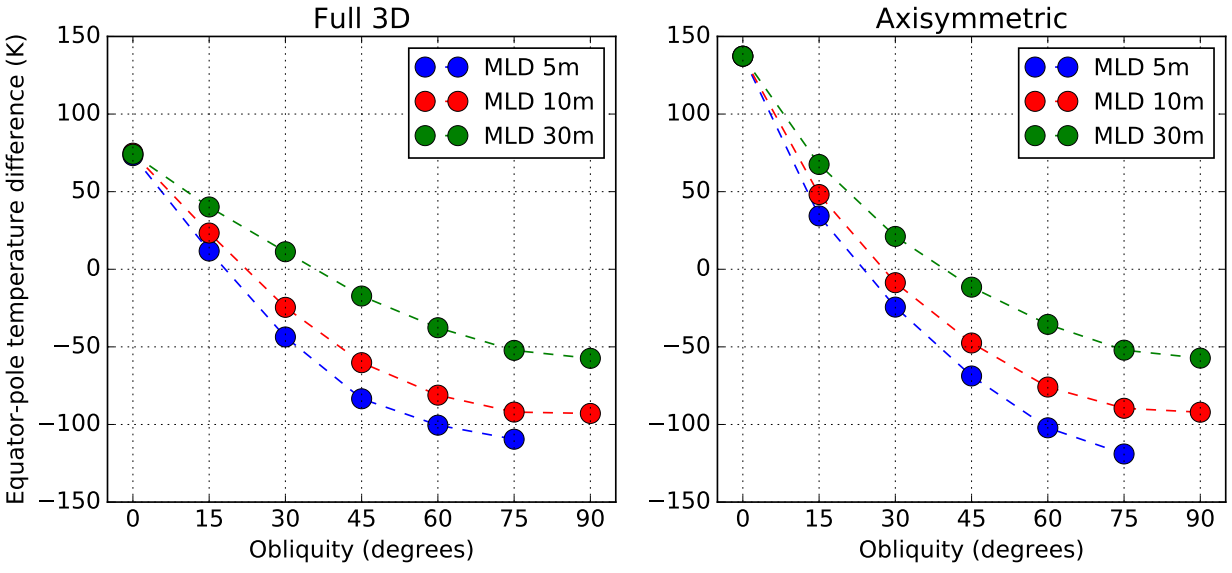

186 FIG. 10. Solstice equator-pole temperature difference in the summer hemisphere, for full 3D eddy permitting,
187 and axisymmetric obliquity variations.

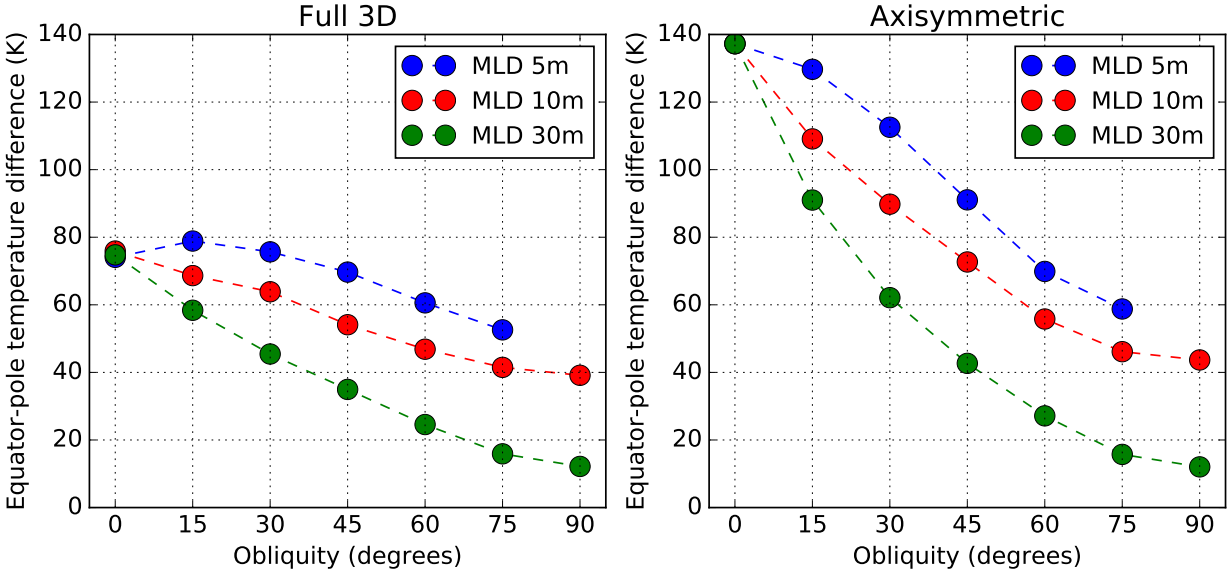

FIG. 11. Solstice equator-pole temperature difference in the winter hemisphere for full 3D eddy permitting, and axisymmetric obliquity variations.

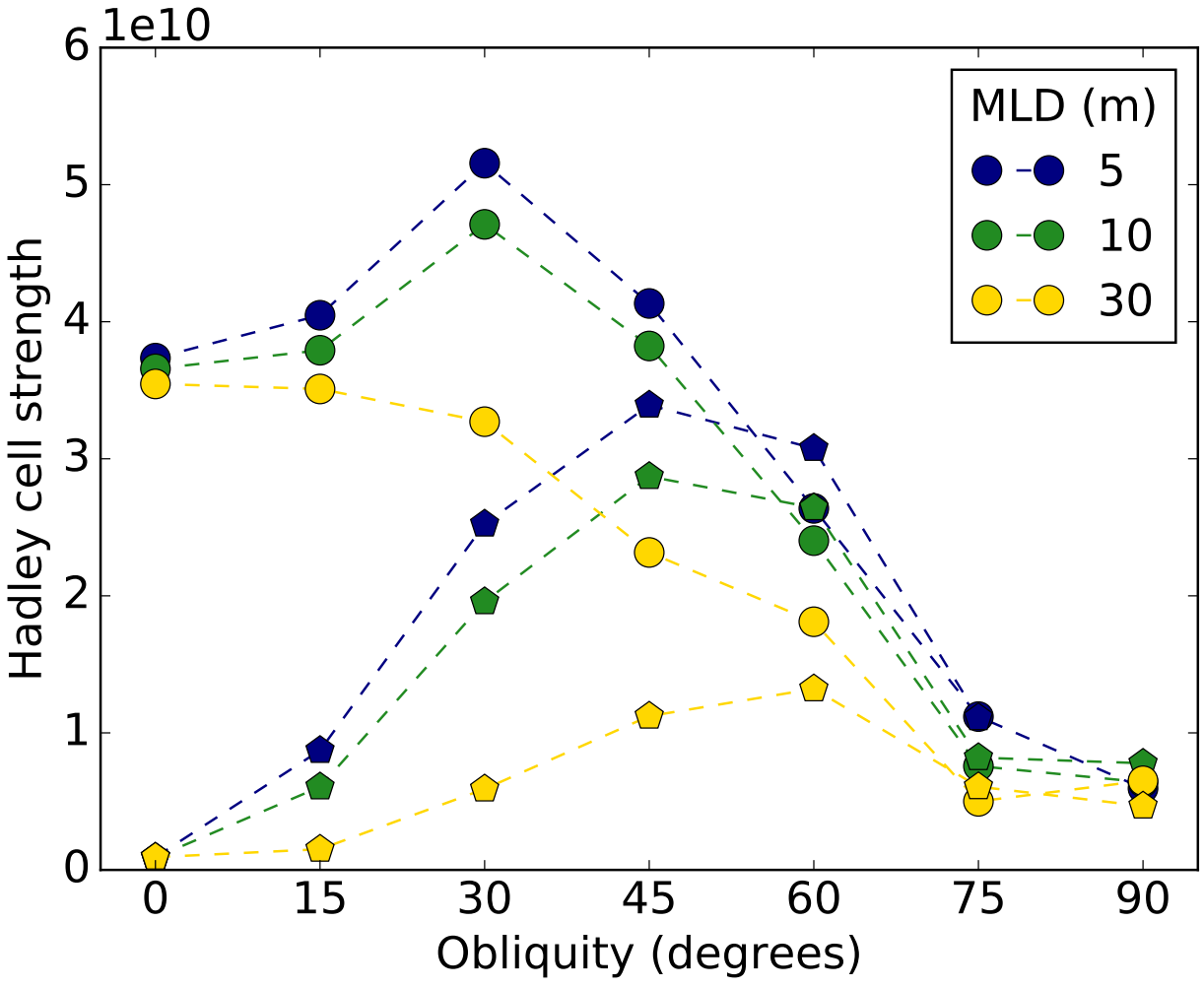

FIG. 12. Annual mean Hadley cell strength for mixed layer depth 5, 10, 30m.

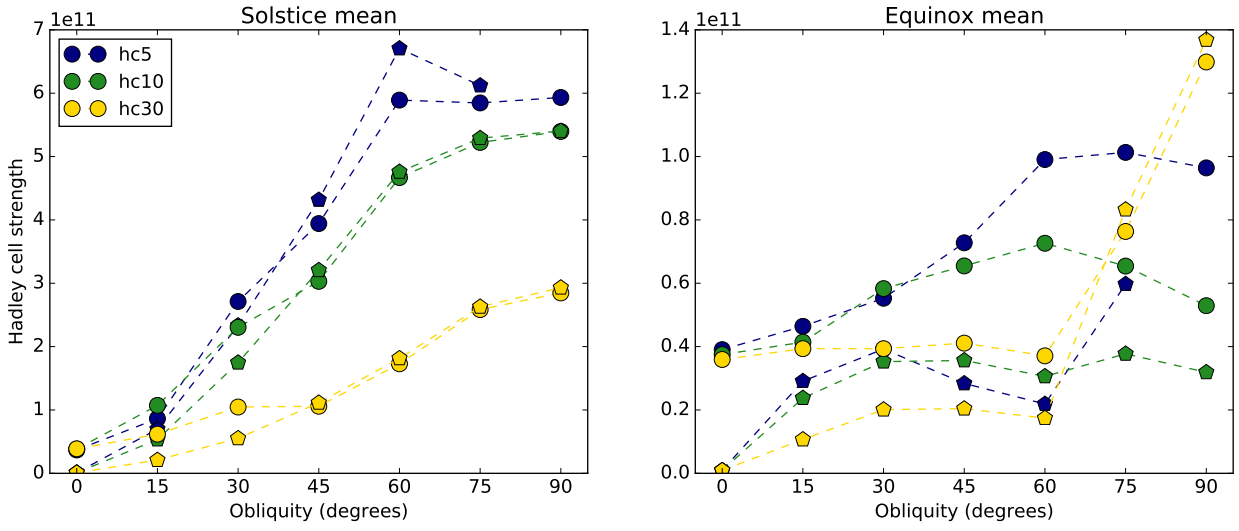

FIG. 13. Seasonal mean Hadley cell strengths for mixed layer depth 5, 10, 30m.

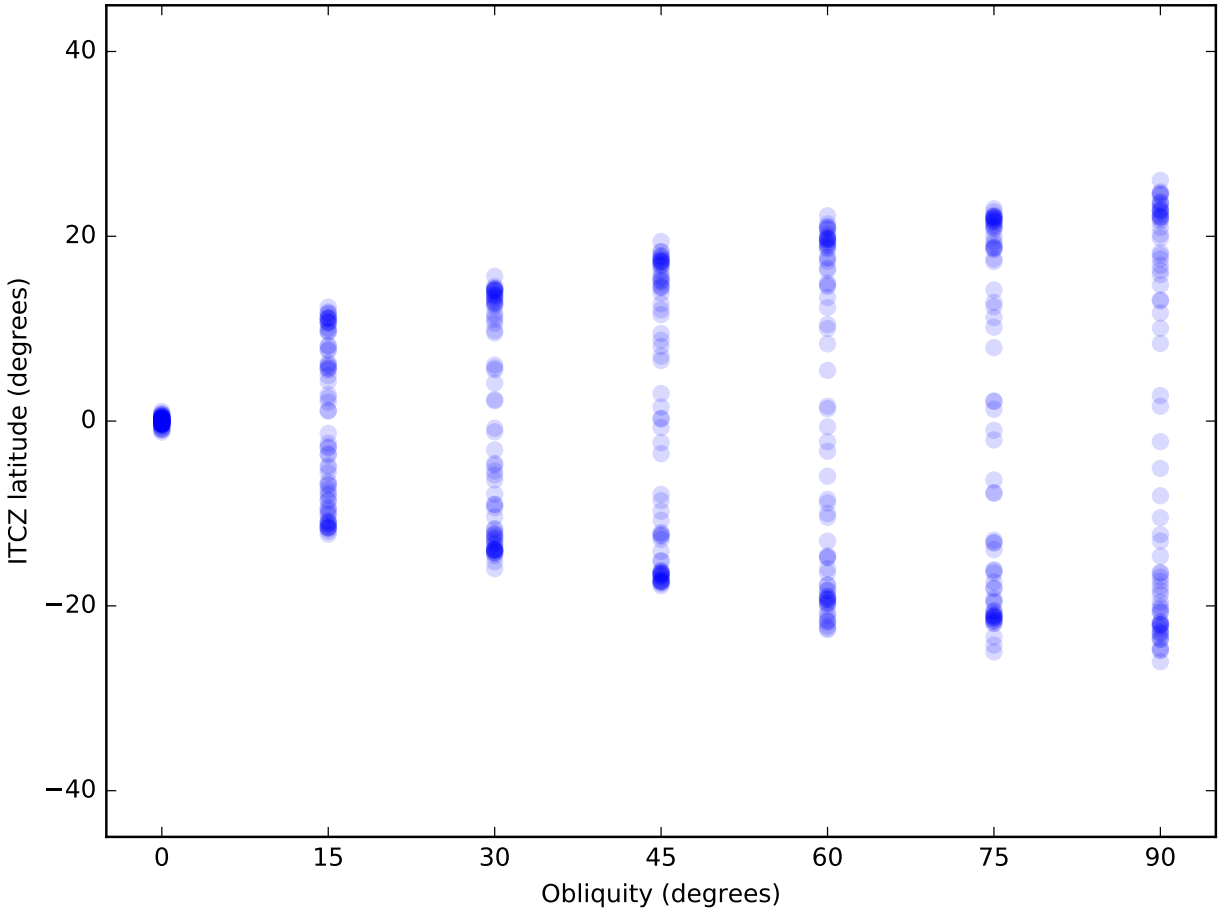

FIG. 14. 5-day mean latitude of the ITCZ for experiments with a mixed layer depth of 10m. We see a strong initial trend when obliquity is first introduced, and slow growth in the outer limit of the ITCZ for any further obliquity. This outer limit is also much less than the obliquity of the planet, only reaching 25 degrees with a 90 degree obliquity.

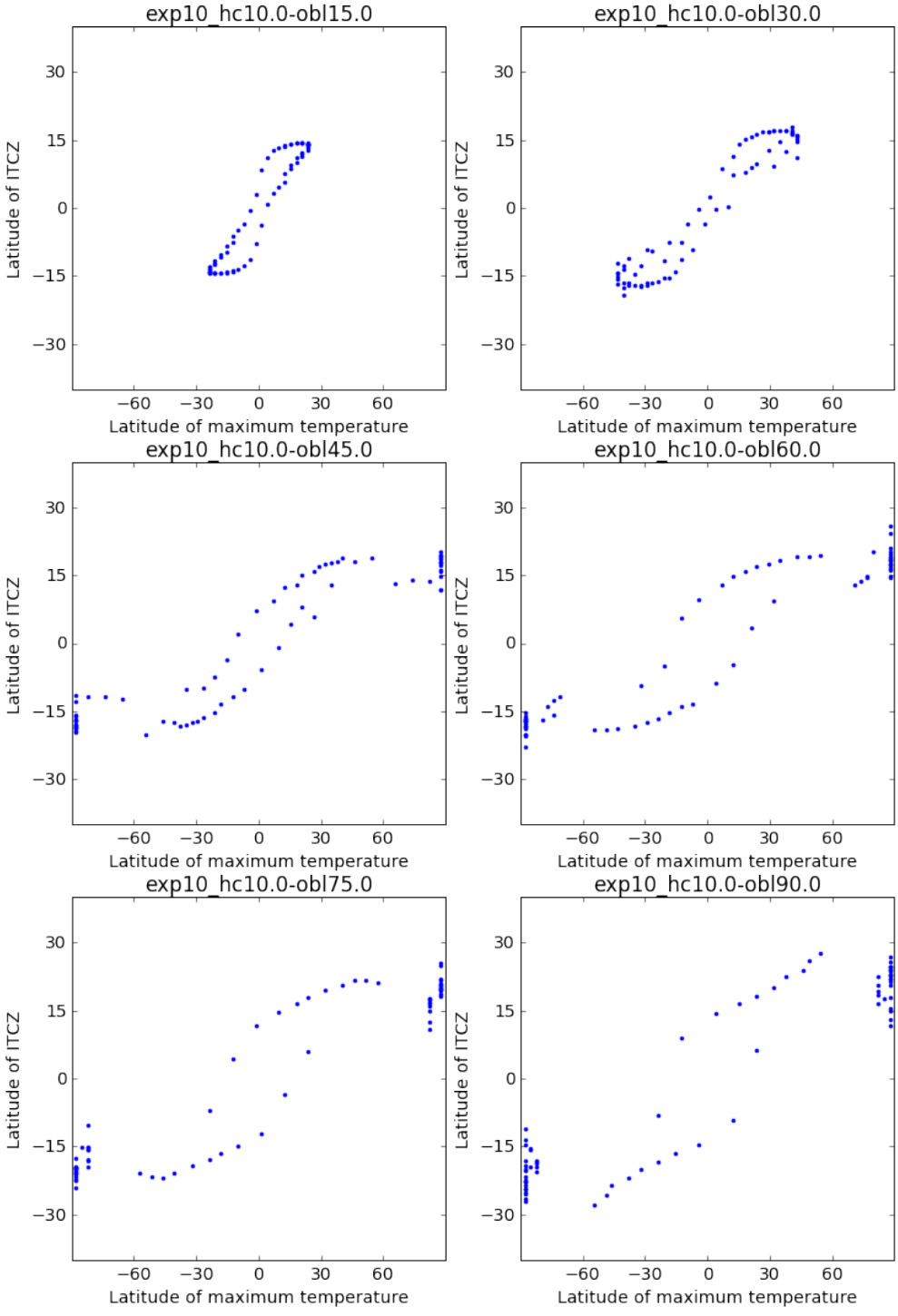
exp10_hc10.0-obl15.0
exp10_hc10.0-obl30.0
exp10_hc10.0-obl45.0
exp10_hc10.0-obl60.0
exp10_hc10.0-obl75.0
exp10_hc10.0-obl90.0
Latitude of ITCZ
Latitude of maximum temperature
30
15
0
−15
−30
−60
−30
0
30
60

FIG. 15.

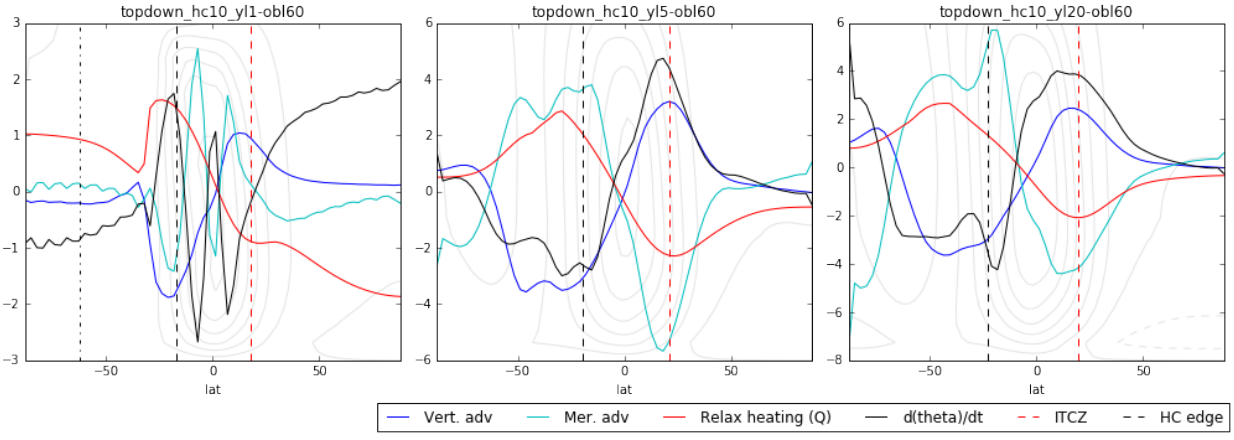

FIG. 16. Solstice mean thermodynamic breakdown of year length varying experiments.